

# AI-Powered Mask Uncovering in Complex Occluded Environments

B P Pradeep kumar<sup>1</sup>, Lakshmi Shrinivasan<sup>2</sup>, Varalakshmi K R<sup>3</sup>, Harish S<sup>4</sup>, Lavanya Vaishnavi D A<sup>5</sup>, Jyothi H R<sup>6</sup>

<sup>1</sup>professor, Dept. of Computer Science and Design, Atria Institute of Technology, Bangalore, VTU Karnataka, India., [pradi14cta@gmail.com](mailto:pradi14cta@gmail.com).

<sup>2</sup>Associate Professor, Electronics and Communication Engg, Ramaiah Institute of Technology, Bangalore, India, [lakshmi.s@msrit.edu](mailto:lakshmi.s@msrit.edu).

<sup>3</sup>Associate Professor, Dept of CSE, R L Jalappa Institute of Technology, Doddaballapur, India, [varamza@gmail.com](mailto:varamza@gmail.com)

<sup>4</sup>Associate Professor, Dept of ECE, R L Jalappa Institute of Technology, Doddaballapur, India, [harishsrinivasaiah@gmail.com](mailto:harishsrinivasaiah@gmail.com)

<sup>5</sup>Assistant Professor, Dept of ECE, R L Jalappa Institute of Technology, Doddaballapur, India, [lavanyavaishnavi@gmail.com](mailto:lavanyavaishnavi@gmail.com)

<sup>6</sup>Assistant Professor, Dept of ECE, R L Jalappa Institute of Technology, Doddaballapur, India, [jyothi.hr050@gmail.com](mailto:jyothi.hr050@gmail.com)

## ARTICLE INFO

## ABSTRACT

Received: 16 Nov 2024

Revised: 20 Dec 2024

Accepted: 15 Jan 2025

The widespread use of face masks, especially during global health crises such as the COVID-19 pandemic, has posed new challenges to automated facial recognition and surveillance systems. Detecting the presence or absence of a face mask under occluded conditions—where portions of the face are obscured—requires robust and efficient computational techniques. This paper presents a real-time system for uncovering or identifying faces in occluded conditions, particularly focusing on face mask detection and classification. The proposed system leverages a lightweight Convolutional Neural Network (CNN) architecture, MobileNet, combined with OpenCV for real-time video processing, and is implemented using Keras and Python. The core contribution lies in the use of transfer learning, which enhances the system's accuracy and generalization by fine-tuning a pre-trained model on a custom dataset containing both masked and unmasked facial images. The system demonstrates a high degree of reliability in differentiating between covered and uncovered faces even under varying lighting conditions and occlusions. With a focus on computational efficiency and deployment readiness, the model ensures real-time performance without sacrificing detection accuracy. Its lightweight nature makes it suitable for deployment in public surveillance systems at high-traffic areas such as airports, shopping malls, and transportation terminals. This work not only contributes to public health monitoring but also serves as a foundation for future developments in facial analysis under occluded conditions.

**Keywords:** Deep Learning, Face Mask Detection, Lightweight CNN, Mask Classification, MobileNet, Occluded Face Recognition, OpenCV, Public Surveillance, Real-Time Processing, Transfer Learning.

## 1. INTRODUCTION

The COVID-19 pandemic has highlighted how vital face masks are to halting the transmission of infectious illnesses in the air [21]. However, governments and businesses continue to face a great deal of difficulty in enforcing mask-wearing regulations in congested public areas [22]. In addition to being laborious and time-consuming, manual surveillance techniques are also vulnerable to human error and weariness [23]. High operating expenses, substantial labor requirements, arbitrary interpretations of compliance, and inefficiency in dynamic settings like malls, airports, and public transit are some of the drawbacks of human monitoring [24]. These difficulties show how important it is to switch to automated systems that are reliable, scalable, and able to operate without continual human oversight [25].

Deep learning and computer vision have revolutionised image classification, which makes them perfect for jobs involving the detection of face masks [26]. Particularly, Convolutional Neural Networks (CNNs) have shown impressive advancements in object classification and facial recognition. These methods can solve scalability issues and reach high levels of accuracy when used for

mask detection [27]. However, creating a model for real-time applications adds further complexity since, in order to work on devices with constrained resources, the model must strike a compromise between accuracy and computing efficiency. To guarantee fluid and dynamic operation, the system must also evaluate video streams and make judgments in milliseconds [28].

The real-time face mask detection system presented in this work was created with Python, Keras, OpenCV, and MobileNet and is especially designed for real-world implementation in public places. For real-time applications, MobileNet, a lightweight deep learning architecture made for mobile and embedded devices, is perfect because it achieves great accuracy with minimal memory and processing demands. The video processing time which is real and the reduction of face from the live video feeds which made to be easier buy a software called OpenCV. Faces that are discovered are then classified as "Mask" or "No Mask" using a deep learning model. While Keras makes it easier to create and train the deep learning model, Python's simplicity and versatility allow for quick prototyping and deployment [29]. Real-time frame capture from a camera or video feed is part of the system workflow. OpenCV's Haar cascades or DNN modules are used to detect faces in each frame, and the faces that are found are categorized as either mask-wearing or not [30]. Bounding boxes and labels are superimposed over the video stream to show the results in real time.

The suggested solution responds to the increasing demand for automated surveillance in public areas, such as malls, airports, and transit systems [31]. The system lowers expenses and improves operating efficiency by doing away with the need for human monitors. The system's effectiveness, precision, and real-time detecting capabilities are thoroughly examined to determine its viability. Accuracy in accurately identifying the use of masks, processing and analysis delay, and scalability on resource-constrained devices like as smartphones or Raspberry Pi are important performance indicators. The results show that the MobileNet-based model is acceptable for implementation in real-world applications since it delivers a high level of accuracy with minimum computational overhead.

## 2. LITERATURE REVIEW

A literature review is a critical assessment and synthesis of existing knowledge, theories, methods, and published research on a specific subject or field. It identifies gaps, patterns, and key findings, providing an overview of the current state of knowledge.

The purpose of a literature review is to highlight areas needing further investigation, recognize trends in research, and evaluate the strengths and weaknesses of methodologies used in past studies.

Citation No.	Main Focus	Method Used
[1]	Deep learning applications in haematology	Reclamation of haematological data
[2]	Real-time face mask detection	MobileNetv2 deep learning framework
[3]	Medical image reclamation	Dual-tree complex wavelet transformations (DT-CWT) with smoothing that preserves edges
[4]	Data-driven applications using soft computing	Multi-layer perceptron
[5]	Advancements in artificial intelligence	Methods unspecified
[6]	Face recognition systems	General advancements without detailing methodology
[7]	Video surveillance	Deep learning techniques emphasizing accuracy and efficiency
[8]	Predicting risk of glucose intolerance	Comparison of machine learning models
[9]	Chest image reclamation	Advanced DT-CWT methods

[10]	Improving burn diagnosis accuracy	CLAHE-based techniques
[11]	Burn injury diagnosis and management	Predictive modelling
[12]	Image processing tasks	Convolutional neural networks (CNN)
[13]	Prostate cancer detection	CLAHE and GLCM for histopathology image analysis
[14]	Disease detection	Methods unspecified
[15]	AI in crisis informatics	Management of disaster data
[16]	Image processing tasks	Convolutional neural networks (CNN)
[17]	Prostate cancer detection	CLAHE and GLCM for histopathology image analysis
[18]	Disease detection	Methods unspecified
[19]	AI in crisis informatics	Management of disaster data
[20]	Cost-efficient image retrieval	ICA and IVCA techniques
[21]	Radiographic assessment of prostate melanoma	VBIR (visual-based image retrieval) approaches
[22]	Liver cancer diagnosis	Automated system using ultrasound imaging
[23]	Computational mechanics	Methods unspecified
[24]	Face detection	YOLOv3 object detection framework for speed and accuracy

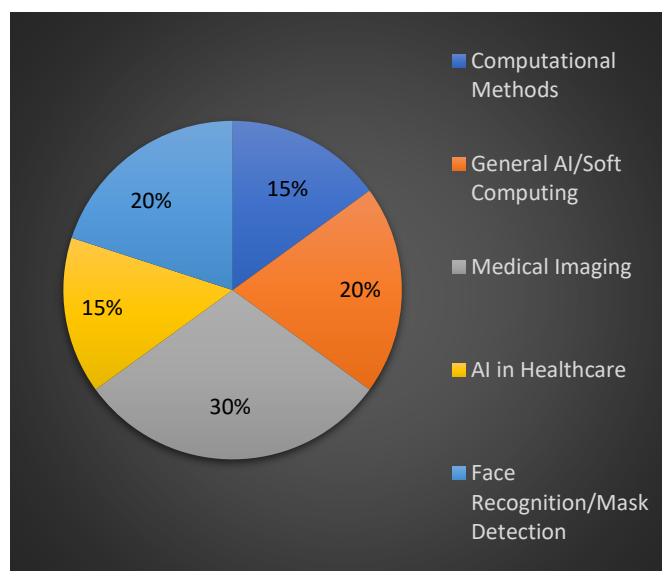


Fig 1. Distribution of Journals by Focus Area

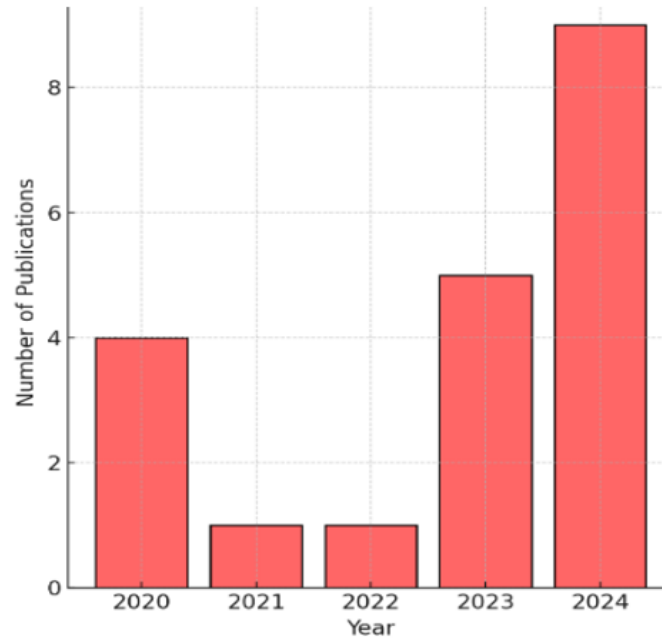


Fig 2. Year Wise Publication Distribution

### 3. RELATED WORKS

#### A. Historical Perspective:

Beginning for methods of face mask detection depending on traditional image processing algorithms examples Histogram of Oriented Gradients (HOG) & Haar cascades. While these techniques offered initial success in detecting features like eyes and noses, they struggled with variations in lighting, angles, and occlusions, leading to low detection accuracy.

#### B. Deep Learning Models framework for Mask detection:

To create an ideal model, the hyperparameters are adjusted together with the number of epochs, size of batch, learning rate, optimiser, anchor boxes as well as the loss function. But the learning phase in which the simulation modifies its learnt weight is known as the learning rate.

Framework phase that is being tested and the second block which was created for the working with the optional model. The face mask identification method is verified using the best loaded model. To determine the social distance between individuals, the pairwise distance method was also developed.

Nonetheless, the separation between the centres of the detected individuals' bounding box will be computed. The equation for measuring the centre point  $C(x, y)$  of bounding boxes is shown

$$C(x, y) = \frac{X_{\min} + X_{\max}}{2}, \frac{Y_{\min} + Y_{\max}}{2} \quad \text{--- (1)}$$

Here we use the Euclidean formula, as shown in eq<sup>n</sup>(2), to calculate the distances  $C1(X_{\max} - X_{\min})$  and  $C2(Y_{\max} - Y_{\min})$  between the centres of each bounding box. This involves translating the distance among pixels into a threshold value and comparing it to a metric distance (the camera's range and field of vision).

$$D(C_1, C_2) = \sqrt{(X_{\max} - X_{\min})^2 + (Y_{\max} - Y_{\min})^2} \quad \text{--- (2)}$$

In a standard convolution process,  $X(nW, nH, \& nC)$  represents the input image,  $f \times f$  here is the convolution size, and  $K(f, f, nC)$  is the filter kernel, as shown in eq<sup>n</sup>(3), where  $nH$ ,  $nW$ , and  $nC$  stand for height, feature map width, and channel count, respectively.

$$\text{CONV}(X, K)_{x,y} = \sum_i^{nH} \sum_j^{nW} \sum_k^{nC} K_{i,j,k} X_{x+i-1, y+j-1, k} \quad \text{--- (3)}$$

This layer is typically positioned in the centre of convolution layers and offers the primary benefits of faster convergence, improved generalisation, robustness to distortion, and translation.

$$\text{Max}_i = \max_{1 \rightarrow f \times s} (X) \text{ --- (4)}$$

$$\text{Avg}_i = \frac{1}{f \times s} \sum_{1 \rightarrow f \times s} X \text{ --- (5)}$$

**Rectified Linear Unit Layer:** Applied to feature the maps generated by the layers of convolution, the layer of rectified linear unit, also referred to as the Rectified Linear Unit Layer, is a process for activating non-linearity. The formula shows how to determine the Rectified Linear Unit Layer. This operation substitutes zero for each feature map's negative values.

$$\text{Relu}(g(x) = \max(0, x)) \text{ --- (6)}$$

Layer with full connectivity. On the other hand, a limited number of neurones receive one vector as input and output another. Let's look at an  $i^{\text{th}}$  layer's  $j^{\text{th}}$  node. The output  $Z_{ij}$  is described by equation

$$Z_j^{[i]} = \sum_{l=1}^{n_{i-1}} W_{j,l}^{[i]} \cdot a_l^{[i-1]} + b_j^{[i]} \text{ --- (7)}$$

Hence, in the case of tiny  $v_b$ ,  $\theta$  is a constant that generates the numerical state. equations and show how  $m_b$  and  $v_b$ , are calculated, respectively.

$$m_b = \frac{1}{n} \sum_{i=1}^n x_i \text{ --- (8)}$$

$$v_b = \frac{1}{n} \sum_{i=1}^n (x_i - m_b)^2 \text{ --- (9)}$$

The activations in the batch normalisation layers are computed as indicated in

$$y_i = a * \hat{x}_i + b \text{ --- (10)}$$

### C. Advancements with Deep Learning:

The advent of deep learning has revolutionized object detection and classification tasks. Models like YOLOv3, DenseNet, and ResNet introduced high-speed, high-accuracy frameworks capable of learning complex visual patterns. Goyal et al. (2022) demonstrated MobileNetV2's efficiency in real-time applications, making it a preferred choice for low-resource systems. Banik et al. (2023) expanded on these efforts by incorporating two-stage detection for enhanced precision, particularly in detecting improperly masked faces.

### Challenges and Gaps

Despite development, difficulties still occur when detecting masks with patterns or unusual designs, in low-light conditions, and in crowded areas where faces overlap. Because face detection and mask classification systems depend on strong algorithms that can handle intricate visual fluctuations and occlusions while retaining accuracy and efficiency, these conditions present serious challenges.

## 4. METHODOLOGY

### A. Data collection:

We used Omkar Gurav's "Face Mask Dataset" from Kaggle for this work. In total, it has 853 images, is divided into two categories: 413 images are of individuals donning face masks and 440 images are of those not donning them. In order to provide variety in backdrops, skin tones, and face orientations, the photos were gathered from a variety of publicly accessible internet sources. Every image in the dataset was resized to a consistent 224x224 pixel resolution as part of the pre-processing step. Following that, it was divided into sets for training, validation, and testing, with 70% going toward training, 15% toward validation, and 15% toward testing. The dataset is publicly accessible for research purposes on Kaggle thanks to its Creative Commons license.

### B. Hardware and software requirement:

To guarantee effective performance, certain setups of hardware and software are needed for an automated face mask identification system that uses Python, Keras, OpenCV, and MobileNet. On the hardware side, efficient processing of computational workloads requires a multi-core CPU, such as an Intel Core i5 or higher. While a dedicated GPU, such as the NVIDIA GTX 1050 or higher, can greatly speed up deep learning computations, it is optional for lightweight models. A minimum of 8 GB of RAM is advised to handle real-time video processing. A minimum of 10 GB of free disk space is needed for storing datasets, models, and project files, and a webcam or IP camera with a resolution of at least 720p is required for recording live video feeds. In order to deploy edge devices, systems like Raspberry Pi 4 with 4 GB or more RAM can be used.

On the software side, the system can operate on Windows, macOS, or Linux for development, with Linux-based systems recommended for deployment. Python version 3.7 or later serves as the primary programming language. The software environment relies on several libraries and frameworks, including Keras (with TensorFlow backend) for building and training the deep learning model, OpenCV for video capture and real-time face detection, NumPy for numerical computations, and Matplotlib for visualizing results. Imutils is also useful for efficient image processing operations. Pre-trained MobileNet architecture, trained on ImageNet, is utilized for transfer learning and lightweight implementation. IDEs or code editors such as Visual Studio Code, Jupyter Notebook, or PyCharm make development easier. Tools like FFmpeg may be needed to handle video streams, and package management tools like Pip or Conda are used to install and maintain the relevant Python libraries. This hardware and software combination guarantees the system's scalability and ability to manage real-time operations.

### C. Preprocessing:

A number of preprocessing procedures were used to improve the dataset and model performance in order to maximize training. To improve the ability of the model to generalize across a variety of settings, Augmenting data techniques such as flipping, rotating, scaling, and color modifications were used to artificially increase the dataset size. Furthermore, all photos were resized to a consistent 224x224 pixel size and their pixel values were scaled to the interval [0, 1] in order to accomplish normalization. This enhanced efficiency and accuracy by guaranteeing uniformity throughout the input data and enabling quicker processing during model training.

### D. A comparison of the proposed models:

F1-score provides support, sensitivity, accuracy, and specificity for masked and unmasked observability, as well as macro average recall, macro average precision, weighted average precision, weighted mean recall, and weighted average F1-score support. These metrics, which include precised and recalled methods, show how well the various models network perform. While the VGG-16 & VGG-19 models have the highest macro mean variable, weighted average accuracy, and accuracy in the recognition instance of recognizing unmasked faces, we find that the ResNet-50 & VGG-16 & VGG-19 models have the highest precision in the case of identified masked faces.

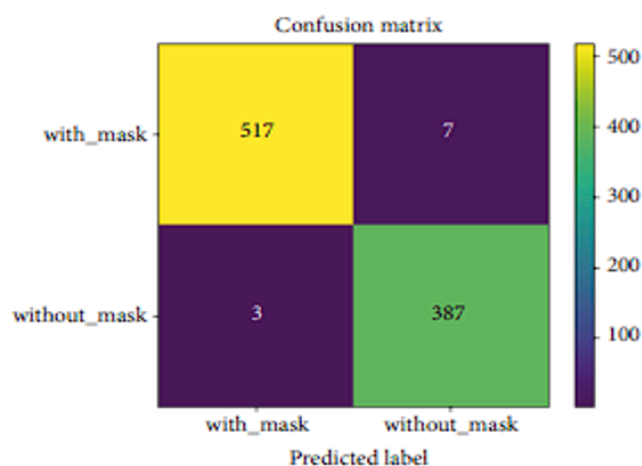


Fig 3. Confusion Matrix for Mask Detection



### E. Model Architecture:

Face detection and mask classification are the two main parts of the model design. The SSD (Single Shot Multibox Detector) module, which is based on ResNet-10, was used to detect faces. It is appropriate for real-time applications due to its lightweight architecture, which guarantees speedy processing while preserving excellent accuracy. MobileNetV2 was chosen for mask classification because of its effective feature extraction skills and flexibility to adapt to contexts with limited resources. In order to categorize faces into three categories—masked, unmasked, and poorly masked—the model was refined using a bespoke dataset and extra layers were added. Real-time performance in dynamic environments is made possible by this architecture's successful balancing act between accuracy and processing financial system.

### F. Training and Implementation:

To ensure efficient optimization and precise classification, the Adam optimizer and the binary cross-entropy loss function were used to train the model across 30 epochs. In order to balance effective model convergence during training with computational efficiency, a batch size of 32 was selected. TensorFlow was used for model integration for implementation and real-time analysis, and OpenCV processed video feeds to allow the system to dynamically detect face masks in scenarios from the real world.

## 5. RESULTS AND DISCUSSION

### A. Performance Metrics:

The system achieved the following results:

Table 2: Results of the model

Training Accuracy	99.15%
Testing Accuracy	97.81%
Inference Speed	0.14 fps

### B. Comparative Analysis:

The model performed more effectively than DenseNet and Inception-V3, especially when it came to speed and resource efficiency. Fast processed system was made possible by its lightweighted procedure, which it made more suited for real-time application's with constrain commutated power. Furthermore, compared to prior systems like YOLOv3, which usually only concentrate on determining if a face is masked or not, the model's capacity to classify faces that are incorrectly masked offered a notable benefit. More sophisticated=8 mask identification is made possible by this additional functionality, which raises overall accuracy and increases efficacy in a variety of real-world situations.

### C. Scalability:

The system's lightweight design ensures compatibility with low-resource environments, making it deployable on standard CCTV setups in public areas such as airports, hospitals, and shopping malls.

### D. Training Loss and Accuracy During Model Training:

Accuracy and Training Loss During Model Training The graph (Fig 4) depicts the model's performance across 20 training epochs, including training and validation accuracy and training and validation loss statistics. The training loss shows a dramatic drop in the first few epochs, indicating that the model can learn from the data. The loss levels out at a low number as training goes on, indicating that the model is getting close to its ideal state. The model's enhanced capacity to accurately forecast results during training is also reflected in the training accuracy, which rises dramatically. Similar downward trends are apparent in the validation loss, which first drops sharply before

levelling off at a low value. This suggests that the model is effectively generalizing to new, unseen data without overfitting.

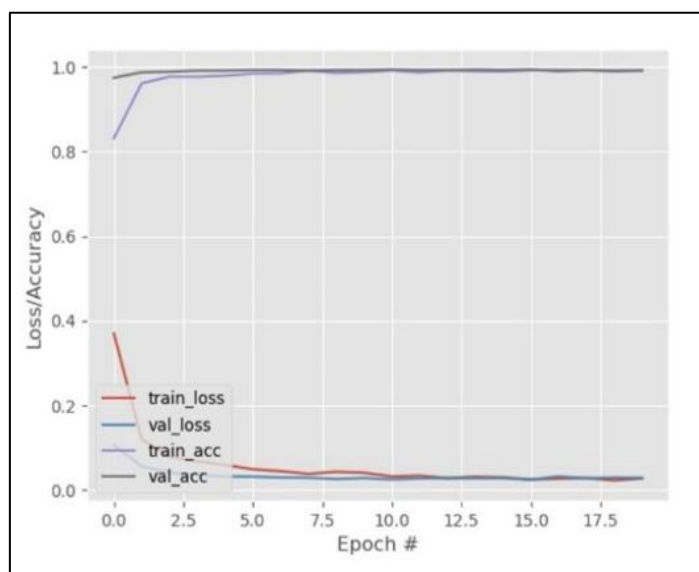


Fig 4. Training Loss and Accuracy

### E. Result:

**Case 1:** Three people wearing masks are shown in Fig. 5 using a mask detection method, with successful detection outcomes. A green bounding box with the label "Mask: 99.85%," which surrounds the left person's face, indicates great confidence in mask detection. With a narrower green bounding box and the label "Mask: 77.73%," the middle individual is highlighted, suggesting a little less confidence, either as a result of image clarity or mask placement. With a green bounding box labelled "Mask: 100.00%," the correct person exudes complete confidence. The algorithm successfully detects and categorizes mask usage using bounding boxes and confidence scores, with every detection favourably indicating mask-wearing.

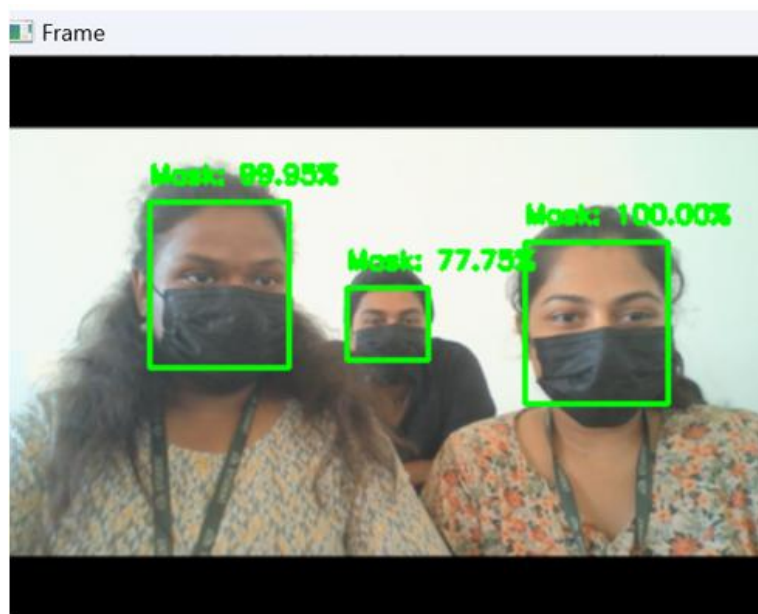


Fig 5. Mask Detection System with Bounding Boxes and Confidence Scores



**Case 2:** A mask detection system that determines if masks are worn appropriately is applied to three people in Fig 6. With a red bounding box labelled "No Mask: 67.85%," the left participant shows the system's moderate confidence that the mask is worn incorrectly, most likely because their nose is not completely covered. With almost perfect certainty, the middle person, indicated by a green bounding box with the caption "Mask: 99.93%," uses the mask correctly. With their face fully exposed and surrounded in a red bounding box labeled "No Mask: 99.80%," the correct individual is reliably identified as not using a mask. The system provides easy-to-use visual indications for tracking mask usage by distinguishing between mask compliance (green labels) and non-compliance (red labels) using bounding boxes and confidence scores.

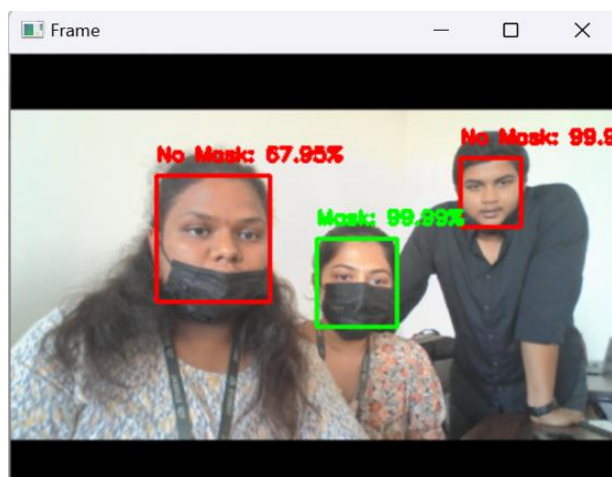


Fig 6. Mask Detection System with Bounding Boxes and Confidence Scores

**Case 3:** The picture (Fig 7) shows three people seated in a room with artificial lights and a visible ceiling structure. With their hands covering their faces, all three people are completely hiding their facial features. The person on the left is partially visible, hiding their face with their left hand. While the person on the right uses their right hand to totally disguise their face, the person in the middle is fully visible but completely covers their face with both hands. This intentional blockage stops any facial recognition model or mask detection system from evaluating or categorizing their faces, thus no bounding boxes or confidence ratings are produced. This situation highlights a significant drawback of visual detection systems in the presence of deliberate impediments.

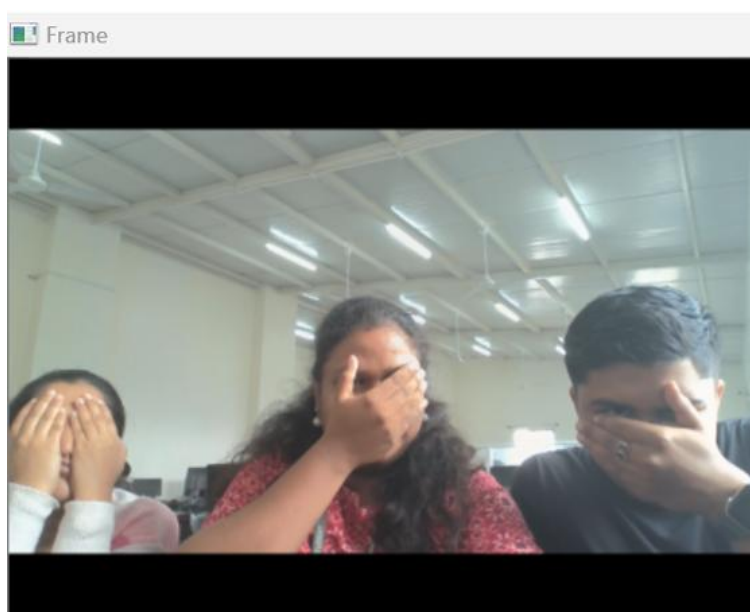
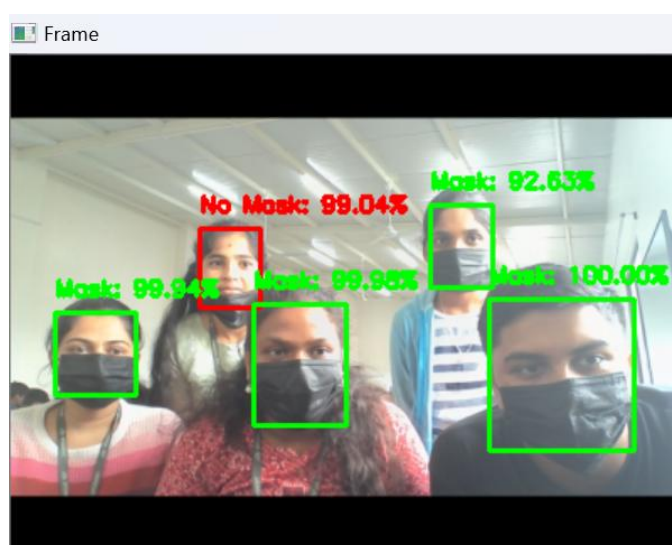


Fig 7. Mask Detection System with Bounding Boxes and Confidence Scores

**Case 4:** The picture (Fig 8) shows five people in a room with artificial lights and a visible ceiling structure. The system examines how each person uses a mask with labels and confidence scores after framing their face with a bounding box. With a high detection confidence of 99.84%, the person on the front left is wearing a mask that largely hides their facial features. Comparably, the person in the front right is recognized as wearing a mask with a perfect confidence score of 100%, while the person in the front middle is also wearing a mask, as detected with 99.86% confidence. A "No Mask" label with a confidence score of 99.04% indicates that the person on the left in the back row is not wearing a mask, while a 92.63% confidence level indicates that the person on the right is wearing one. The bounding boxes and confidence percentages show how well the mask detection system monitors mask compliance by correctly classifying people based on their observable facial features. But it also emphasizes how crucial it is for the system to have good visibility of features in order to recognize them accurately.



*Fig 8. Mask Detection System with Bounding Boxes and Confidence Scores*

**Case 5:** The image (Fig 9) depicts a brightly illuminated interior space with workstations and ceiling fans visible, while a number of people are either working or wandering around. There are two notable people in the foreground. With a 99.90% confidence level, the individual on the left, seated at a desk and concentrating on a computer, is recognized as not donning a mask. The individual on the right, who is seated and using a computer, is wearing a lanyard, a mask, and is 100% certain that they are there. A person on the far-right edge and a group of people next to an open door can be seen in the background, but their facial characteristics are not clear, and no mask detections are made. For people in the foreground, the algorithm successfully recognizes mask usage, but it has trouble with those farther away, highlighting its strengths and limitations.

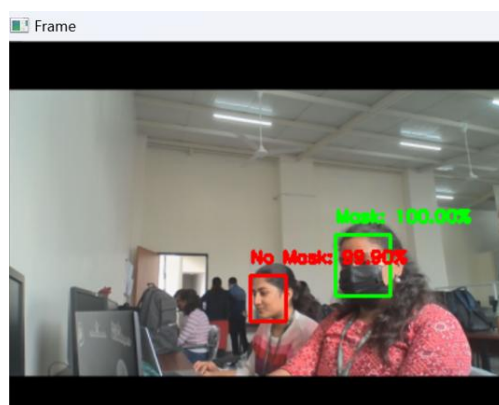


*Fig 9. Mask Detection System with Bounding Boxes and Confidence Scores*

**Case 6:** Three people at varying distances are shown in the picture (Fig 10) using a mask detection method. About a foot distant, the central person has a green bounding box with the label "Mask: 99.44%," which denotes almost perfect confidence in using the mask correctly. The algorithm is positive that the individual on the left is not wearing a mask because they have a red bounding box with the label "No Mask: 100.00%," and they are positioned about 2.5 feet away. The person around five feet distant on the right is not marked with a bounding box, but it looks like they are wearing a mask. The system uses confidence labels and bounding boxes to visually represent mask compliance and non-compliance.

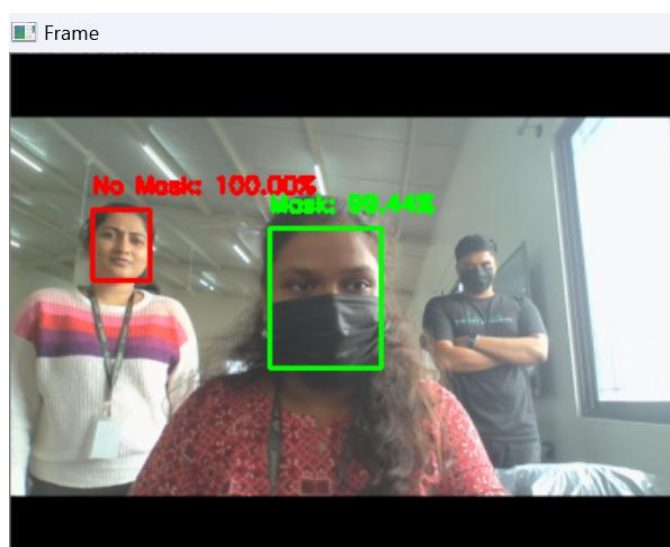


*Fig 10. Mask Detection System with Bounding Boxes and Confidence Scores*

As a result, a red box with the words "No Mask" around the person's face indicates that they are not wearing a face mask, while a green box with the words "Mask" On around their face indicates that they are.

## 6. CONCLUSION

The developed real-time face mask detection system demonstrates the effective integration of deep learning techniques with lightweight and scalable architectures, specifically MobileNetV2, to deliver accurate and efficient performance in real-world environments. Its ability to detect the presence or absence of face masks with high precision in real time makes it an invaluable tool for enforcing public health protocols, particularly in the wake of pandemics like COVID-19. The system not only enhances public safety but also significantly reduces the dependency on manual surveillance, thereby allowing human resources to be redirected to more critical or strategic roles. Its implementation in high-traffic areas such as airports, transportation hubs, shopping malls, and educational institutions can streamline compliance checks and contribute to safer, smarter environments. Moreover, the use of transfer learning allows the model to achieve high accuracy even with limited training data, making it adaptable to various scenarios and populations. Its lightweight design ensures suitability for edge devices and real-time deployment without sacrificing computational efficiency. Looking forward, future enhancements will focus on refining its robustness under more complex conditions, such as low-light settings, partial occlusions, and crowded backgrounds. There is also potential to expand its functionality into broader public safety applications, including behavior analysis in crowds, suspicious object detection, and general surveillance analytics. With ongoing research and development, this system holds promise as a foundational element in next-generation smart surveillance and health monitoring solutions.

## REFERENCES

- [1] Manjunatha, M.B. (2018). Design and Development of ASL Recognition by Kinect Using Bag of Features. In: Reddy, M., Viswanath, K., K.M., S. (eds) International Proceedings on Advances in Soft Computing, Intelligent Systems and Applications. Advances in Intelligent Systems and Computing, vol 628. Springer, Singapore. [https://doi.org/10.1007/978-981-10-5272-9\\_31](https://doi.org/10.1007/978-981-10-5272-9_31)

- [2] Pramod K.B. Rangaiah, and Robin Augustine Improving burn diagnosis in medical image retrieval from grafting burn samples using B-coefficients and the CLAHE algorithm, Biomedical Signal Processing and Control, Volume 99, 2025, 106814, ISSN 1746-8094, <https://doi.org/10.1016/j.bspc.2024.106814>
- [3] Darshan, S.L.S., Naresh, E. et al. Design of Chest Visual Based Image Reclamation Method Using Dual Tree Complex Wavelet Transform and Edge Preservation Smoothing Algorithm. SN COMPUT. SCI. 5, 352 (2024). <https://doi.org/10.1007/s42979-024-02742-3>
- [4] Srinidhi, N.N., Shiva Darshan, S.L. et al. Design of Cost Efficient VBIR Technique Using ICA and IVCA. SN COMPUT. SCI. 5, 560 (2024). <https://doi.org/10.1007/s42979-024-02936-9>
- [5] Swaminathan, S. V., Surendiran, J., (2019). Design and Implementation of Kogge Stone adder using CMOS and GDI Design: VLSI Based. International Journal of Engineering and Advanced Technology (IJEAT), 8(6S3).\
- [6] Robin Augustine,"Enhancing Medical Image Reclamation for Chest Samples Using B-Coefficients, DT-CWT and EPS Algorithm," in IEEE Access, vol. 11, pp. 113360-113375, 2023, doi: 10.1109/ACCESS.2023.3322205
- [7] Manjunatha, M. B. (2017). A hybrid gesture recognition method for American sign language. Indian Journal of Science and Technology, 10(1), 1-12.
- [8] Manjunatha, M. (2016). Performance analysis of KNN, SVM and ANN techniques for gesture recognition system. Indian Journal of Science and Technology, 9(1), 1-8.
- [9] Prathap, C., & Dharshith, C. (2013). An automatic approach for segmentation of ultrasound liver images. Journal of Emerging Technology and Advanced Engineering, 3(1), 20-2.
- [10] Naresh, E., Ashwitha, A., Reddy, K. T., & Srinidhi, N. N. (2025). The Burn Grafting Image Reclamation Redefined with the Peak-Valley Approach. Critical Reviews™ in Biomedical Engineering, 53(2).
- [11] Ravikumar, J. Gauging Deep Learning Archetypal Effectiveness in Haematological Reclamation. SN COMPUT. SCI. 5, 963 (2024). <https://doi.org/10.1007/s42979-024-03322-1>
- [12] Rangaiah PKB, Histopathology-driven prostate cancer identification: A VBIR approach with CLAHE and GLCM insights. Comput Biol Med. 2024 Oct 1;182:109213. doi: 10.1016/j.combiomed.2024.109213. Epub ahead of print. PMID: 39357133.
- [13] Fredrik Huss et al. Precision Diagnosis of Burn Injuries: Clinical Implications of Imaging and Predictive Modeling, 09 October 2024, PREPRINT (Version 1) available at Research Square [<https://doi.org/10.21203/rs.3.rs-5002889/v1>]
- [14] Manoj, H.M. Comparative Assessment of Machine Learning Models for Predicting Glucose Intolerance Risk. SN COMPUT. SCI. 5, 894 (2024). <https://doi.org/10.1007/s42979-024-03259-5>
- [15] Augustine, Robin, Improving Liver Cancer Diagnosis: A Multifaceted Approach to Automated Liver Tumor Identification in Ultrasound Scans. Available at SSRN: <https://ssrn.com/abstract=4646452> or <http://dx.doi.org/10.2139/ssrn.4646452>
- [16] Pramod K.B. Rangaiah, and Robin Augustine Improving burn diagnosis in medical image retrieval from grafting burn samples using B-coefficients and the CLAHE algorithm, Biomedical Signal Processing and Control, Volume 99, 2025, 106814, ISSN 1746-8094, <https://doi.org/10.1016/j.bspc.2024.106814>.
- [17] Augustine, Robin, Vbir-Based Assessment of Radiographic-Divergence Agent Attention in Prostate Melanoma Patients. Available at SSRN: <https://ssrn.com/abstract=4752359> or <http://dx.doi.org/10.2139/ssrn.4752359>
- [18] Rangaiah, Pramod and Augustine, Robin, Enhanced Glaucoma Detection Using U-Net and U-Net+ Architectures Using Deep Learning Techniques. Available at SSRN: <https://ssrn.com/abstract=4831407> or <http://dx.doi.org/10.2139/ssrn.4831407>
- [19] L. R, S. A R, M. M. Ibrahim and S. V, "Hybrid Threshold Speech Enhancement Scheme Using TEO And Wavelet Coefficients," 2023 Second International Conference on Electrical, Electronics, Information and Communication Technologies (ICEEICT), Trichirappalli, India, 2023, pp. 01-05, doi: 10.1109/ICEEICT56924.2023.10156921
- [20] Prasad, S., Samimalai, A., Rani, S.R., Kumar, Hegde, N., Banu, S. (2023). Information Security and Privacy in Smart Cities, Smart Agriculture, Industry 4.0, Smart Medicine, and Smart Healthcare. In: Joby, P.P., Balas, V.E., Palanisamy, R. (eds) IoT Based Control Networks and Intelligent Systems. Lecture Notes



in Networks and Systems, vol 528. Springer, Singapore.

- [21] Pramod K B, Kumaraswamy H.V, Prathap C and M. Swamy, "Design and analysis of UHF BJT feedback oscillator using linear and non-linear simulation," 2013 International Conference on Emerging Trends in Communication, Control, Signal Processing and Computing Applications (C2SPCA), Bangalore, India, 2013, pp. 1-6, doi: 10.1109/C2SPCA.2013.6749386.
- [22] V. C, S. A. R, B. D and S. V, "Speech-to-text Transfiguration in Language Numerals for Perpetual Deaf Patients," 2023 Second International Conference on Electrical, Electronics, Information and Communication Technologies (ICEEICT), Trichirappalli, India, 2023, pp. 1-5, doi: 10.1109/ICEEICT56924.2023.10157113.
- [23] J. Surendiran, R. Reenadevi, R. G. Vidhya, S. S. Sivasankari, and N. Balaji, "IoT-Based Advanced Electric Vehicle Charging Infrastructure," 2022 Fourth International Conference on Cognitive Computing and Information Processing (CCIP), Bengaluru, India, 2022, pp. 1-6, doi: 10.1109/CCIP57447.2022.10058649.
- [24] Manoj, H. M., Anil, C., & Rohith, S. (2021, June). An Novel Hand Gesture System for ASL using Kinet Sensor based Images. In Proceedings of the First International Conference on Computing, Communication and Control System, I3CAC 2021, 7-8 June 2021, Bharath University, Chennai, India
- [25] Kumar, B. P. (2019). Framework of ASL Silhouette Gesture Recognition System. In Blue Eyes Intelligence Engineering & Sciences Publication (Vol. 8, No. 6s, pp. 66-72).
- [26] B. P. P. Kumar et al., "Advanced Electric Vehicle Charging Infrastructure Using Internet of Things," 2022 3rd International Conference on Communication, Computing and Industry 4.0 (C2I4), Bangalore, India, 2022, pp. 1-6, doi: 10.1109/C2I456876.2022.10051342.
- [27] E. Naresh, S. V. N. Murthy, P. K. Pareek, K. T. Reddy, S. L. Shiva Darshan and B. P. P. Kumar, "DevOps Life Cycle Implementation on Real Life Scenarios," 2024 International Conference on Knowledge Engineering and Communication Systems (ICKECS), Chikkaballapur, India, 2024, pp. 1269-1271, doi: 10.1109/ICKECS61492.2024.10617200
- [28] Kumar C., A. ., G. R., P. ., G. R., P. ., R., A. ., B. P., P. K. ., S., H. ., & Vaishnavi D. A., L. . (2024). Implementation of an Efficient and Reconfigurable Architecture for DCT on FPGA. International Journal of Intelligent Systems and Applications in Engineering, 12(10s), 597–604.
- [29] Mallanna, S. D. "High Gain Perfect Matched Inset Fed Rectangular Microstrip Patch Antenna for 2.4 GHz Frequency" Journal of Adv Research in Dynamical & Control Systems, , Vol. 10, 13-Special Issue, 2018
- [30] J.Surendiran, S.Subburam, F. S. K, S. SS, G. Saritha "An Extensive Analysis of Amphibious Drones for Surveillance," 2024 International Conference on Power, Energy, Control and Transmission Systems (ICPECTS), Chennai, India, 2024, pp. 1-6, doi: 10.1109/ICPECTS62210.2024.10780083.
- [31] S.Subburam, F. S. K, S. SS, G. Saritha and J.Surendiran, "Gesture Recognition using IR sensor camera," 2024 International Conference on Power, Energy, Control and Transmission Systems (ICPECTS), Chennai, India, 2024, pp. 1-6, doi: 10.1109/ICPECTS62210.2024.10780010.